Alignment creation in atomic ensembles by elastic electron scattering; the case of ^{138}Ba (...6s6p $^1P_1$) atoms

S. Trajmar[†◆], I. Kanik[†‡], M. A. Khakoo[‡], L. R. LeClair[†o], I. Bray[*], D. Fursa[*] and G. Csanak[x]

† *California Institute of Technology, Jet Propulsion Laboratory, Pasadena, CA 91109, USA*

◆ *California Institute of Technology, Division of Chemistry and Chemical Engineering, Pasadena, CA 91109, USA*

‡ *California State University, Department of Physics, Fullerton, CA* 92634, *USA*

* *Electronic Structure of Materials Centre, The Flinders University of South Australia, G.P.O. Box 2100, Adelaide 5001, Australia*

x *University of California, Los Alamos National Laboratory, Los Alamos, NM 87544, USA*

o *Present address: MPB Technologies, Pointe Claire, Quebec H9R 1E9, Canada*

The questions whether elastic electron scattering by initially isotropic atomic ensembles can lead to alignment and to what degree, have been raised recently in connection with plasma polarization spectroscopy by Petrashen et al. (1984), Dashevskaya and Nikitin (1987), Fujimoto (1996) and Kazantsev (1996). For a discussion of plasma polarization spectroscopy, see Kazantsev and Henoux (1995). Until now, there have been no experimental data available to answer these questions and calculations based on various scattering approximations have failed to address these issues.

Here, we describe some of our results from a joint experimental and theoretical program concerning elastic electron scattering by ^{138}Ba (...6s6p $^1P_1$) atoms. From the experimental results, we derived various scattering parameters and magnetic sublevel specific differential elastic scattering cross sections at impact energy (E_0) of 20.0 eV and at scattering angles (θ) of 10°, 15°, and 20°. The same parameters and cross sections were calculated by the convergent close coupling (CCC) approximation and compared to the experimental results. An excellent agreement, found for the two sets of data, gave us confidence in the CCC method and allowed us to extend the angular and energy ranges for the purpose of generating integral elastic scattering cross sections needed for the deduction of the alignment creation cross sections. The integral cross sections needed here are related to the process $^{138}Ba\ (...6s6p\ ^1P_1;\ isotr) + e^-(E_o) \rightarrow {}^{138}Ba\ (...6s6p\ ^1P_1;\ M_f) + e^-(E_o)$ and will be denoted as $Q(M_f)$ where M_f refers to the final magnetic sublevel quantum number. The alignment creation cross section, $Q^{[2]}_{CR}$, for this case is given by Kazantsev et al. (1988) as:

$$Q^{[2]}_{CR} = (2/3)^{1/2}[Q(M_f = 1) - Q(M_f = 0)].$$

Calculations were carried out at E_o = 2.8, 20.0 and 97.8 eV in the full 0° to 180° angular range in one degree steps and the results indicate that alignment can be created to a significant degree by elastic electron scattering.

In the following, we are going to describe briefly the experimental and theoretical methods, show the comparison of some experimental and theoretical results and present the values obtained for $Q(M_f)$ and $Q^{[2]}_{CR}$ as well as several other integral elastic cross sections for the purpose of comparison.

The experimental arrangement has been described earlier by Zetner et al. (1990). A collimated atomic Ba (naturally occurring isotopic mixture) beam was crossed at 90° by a nearly monoenergetic ($\Delta E_{1/2} \approx 0.08$ eV) electron beam. The interaction region was illuminated by a linearly polarized laser beam which was located in the scattering plane and was produced from a ring laser, operating in single mode. The laser wavelength was tuned to excite the ^{138}Ba (...6s^2 $^1S_o \rightarrow$ ...6s6p $^1P_1$) transition. (See Fig. 1 for the energy level scheme.) The elastic scattering signal was measured at a fixed (E_o, θ) for fixed laser geometries, with respect to the laboratory frame (θ_v, ϕ_v), as a function of the linear polarization angle (ψ) with respect to the scattering plane.

The measured count rates in the elastic scattering experiment include contributions from background, from elastic scattering by ground state atoms of all isotopes, and from elastic scattering by coherently excited $^1P_1$

(I_{cP}^{el}) and cascade populated $^3D_2$ and $^1D_2$ metastable ^{138}Ba atoms. In order to assure identical experimental conditions for the modulation measurements, to separate I_{cP}^{el} from other contributions to the measured signal and to obtain various parameters and absolute cross sections from the experiments, we needed to carry out 116 measurements for each fixed (E_0, θ) case. These measurements involved the inelastic ($^1S_0 \rightarrow {}^1P_1$), the superelastic ($^1P_1 \rightarrow {}^1S_0$) and the elastic scattering channels. Scattering intensities for various combinations of the Ba beam and laser beam turned ON and OFF, at two laser positions (laser in the scattering plane and laser displaced by about 4 mm parallel to the scattering plane upstream of the Ba beam) and for four laser geometries ($\theta_v = 45°$ and $90°$, both with $\phi_v = 0°$ and $180°$) were measured and the modulation of the elastic and superelastic scattering intensities as a function of ψ was determined. Normalization of the $I_{cP}^{el}(\psi)$ signal to the corresponding differential cross section, $DCS_{cP}^{el}(\psi)$, was achieved by measuring the ratio of this elastic scattering signal to the signal associated with ($^1S_0 \rightarrow {}^1P_0$) inelastic scattering and utilizing the derived population fractions and the ($^1S_0 \rightarrow {}^1P_0$) inelastic differential cross section values of Wang et al. (1994).

At this stage, we have [for a fixed (E_0, θ) case] a modulation equation of the type

$$DCS_{cP}^{el}(\psi) = \tfrac{1}{4}\, DCS_{P}^{el} \{ A + B \cos 2\psi \}$$

for each laser geometry (Zetner et al., 1990). The values of A and B were obtained from least squares fitting of the experimental data. They contain factors related to the laser geometry and parameters related to the physics of the electron-atom collision. Measurements with several laser geometries were needed to obtain these parameters and various cross sections. We denote here the differential cross sections associated with scattering processes where the initial atomic states are prepared by coherent excitation to the $^1P_1$ state with a particular laser geometry and polarization as $DCS_{cP}^{el}(\psi)$. For differential cross sections associated with processes where the initial and/or final magnetic sublevel is specified (or averaged-over incoherently), we use the notation $DCS_P^{el}(M_i, M_f)$, $DCS_P^{el}(M_i = M)$, $DCS_P^{el}(M_f = M)$ and DCS_P^{el}. Omission of M_i and/or M_f implies averaging (summation) over those magnetic sublevel quantum numbers. M can take the values of -1, 0 or +1. (We select for the quantization axis for the magnetic sublevel cross sections the incoming electron momentum vector.) Since the spin of the scattering electrons was not selected or detected in the present measurements, averaging over initial and summation over final spin quantum numbers are always assumed.

The modulation equation can be used in two different ways: (i) to obtain EICP's and differential cross sections for the hypothetical "inverse" process, i.e. for elastic scattering by an isotropic, incoherent state of ^{138}Ba (...6s6p $^1P_1$) atoms, (ii) to obtain collision parameters and differential cross sections for elastic scattering by the coherently prepared ^{138}Ba (...6s6p $^1P_1$) atoms.

For evaluation of the modulation equations in terms of the hypothetical "inverse" process (based on the

theory of Macek and Hertel,1974), we have for the modulation coefficients (Zetner et al. 1990):

$$A = 1 + \cos^2\theta_n + \lambda(1-3\cos^2\theta_n) + (\lambda - 1)\cos\varepsilon\sin^2\theta_n + \kappa\sin 2\theta_n\cos\phi_n$$

$$B = (3\lambda - 1)\sin^2\theta_n + (1 - \lambda)\cos\varepsilon(1 + \cos^2\theta_n) + \kappa\sin 2\theta_n\cos\phi_n$$

where

$$\kappa = 2\sqrt{\lambda(1-\lambda)}\cos\chi = 2\sqrt{\lambda(1-\lambda)}\cos\Delta\cos\tilde{\chi}\ .$$

In the present experiments, $\theta_n = \theta_v + \theta\cos\phi_n$ and for scattering to the left we have $\phi_v = 180°$ and $\phi_n = \phi_v - \pi = 0°$ and for scattering to the right we have $\phi_n = \phi_v = 180°$. The modulation equations involve the four EICP's (λ, $\cos\varepsilon$, $\cos\Delta$ and $\tilde{\chi}$) as defined by da Paixao et al.(1980) and applied to the Ba superelastic scattering by Zetner et al. (1990). From our laser-in-plane measurements we can extract only λ, $\cos\varepsilon$ and κ. These EICP's can be obtained by solving any set of three equations defining A or B for laser geometries with $\theta_v = 45°$ and 90°. There are 16 meaningful such combinations, each yielding a set of EICP's. We took the average of these 16 sets as our experimental values. Definition of these EICP's and their relations to various cross sections and scattering amplitudes for a ($^1S_0 \leftrightarrow {}^1P_1$) process is given by Zetner et al. (1990). The only difference here is the generalization from the ($^1S_0 \leftrightarrow {}^1P_1$) to the ($^1P_1 \leftrightarrow {}^1P_1$) transition which requires averaging over the initial magnetic sublevels of the $^1P_1$ level. From λ and DCS_P^{el}, we obtained $DCS^{el}(M_f = 0)$. From $DCS^{el}(M_f = 0)$ and DCS_P^{el}, the $DCS^{el}(M_f = 1)$ values were calculated. DCS_P^{el} was obtained by taking the average of $DCS_{\sigma P}^{el}(\psi_m)^+$ and $DCS_{\sigma P}^{el}(\psi_m)^-$ where ψ_m is the polarization magic angle satisfying the condition $\cos 2\psi_m = 1/3$ and the superscript +(-) refers to $\phi_n = 0°(180°)$.

The present e^--Ba scattering calculations have been performed by using the CCC method in the non-relativistic LS-coupling framework (see Fursa and Bray, 1997 and 1998 for details). In brief, the barium atom was considered to have two active valence electrons above an inert Hartree-Fock core. Phenomenological one-electron and two-electron polarization potentials have been added to account for the core polarization. Configuration-interaction (CI) expansions have been used to obtain the Ba wave functions. One electron orbitals have been obtained from the diagonalization of the Ba^+ Hamiltonian in the Sturmian (Laguerre) basis. This allowed us to obtain good description of the Barium discrete states and to achieve square-integrable discretization of the Ba continuum. All negative-energy states (relative to the Ba^+ ground state) and a large number of positive energy states (representing coupling to the ionization continuum) have been included in the CCC calculations.

The total number of states used in the present calculations was 115. They consisted of 14 ^{1}S, 17 ^{1}P°, 19 ^{1}D°, 19 ^{1}F°, 7 ^{3}S, 9 ^{3}P°, 9 ^{3}D°, 9 ^{3}F° and two each of ^{1,3}P°, ^{1,3}D° and ^{1,3}F° states.

Selected values of the large set of the measured and calculated cross sections and parameters are shown in Figs. 2 and 3, respectively. The estimated experimental error limits for these quantities are 30% for the differential cross sections and λ parameter and 40% for the cos ε parameter.

In Fig. 2, three theoretical differential cross sections are shown over the full angular range and compared to the experimental results. The experimental and theoretical results agree well within the estimated experimental error limits. The values for these cross sections drop almost five orders of magnitude between 0° and 70°. It is clear from the present study that the cross sections at high scattering angles are very small and their measurement would be extremely difficult. Therefore, one will have to rely on the theoretical calculations in these regions. A "shoulder" with an inflexion point at around 35° and two deep minima at around 72° and 134° appear in the theoretical curves. The calculations show that the various DCS_P^{el} (M_i, M_f) values differ by more than an order of magnitude but these differences are eliminated, to a large extent, in the averaging processes. The difference in DCS_P^{el} ($M_f = 1$) and DCS_P^{el} ($M_f = 0$) values, which determines the alignment creation cross section, is, however, significant at most scattering angles.

In Fig. 3 the EICP's, λ and cos ε are shown. Not surprisingly, very good agreement between experiment and theory is found for λ since it represents the ratio of two cross sections which both show, separately, good agreement between experiment and theory. Somewhat less satisfactory is the agreement for cos ε. While no significant features appear in the λ curve, the cos ε curve shows a deep minimum at around 22° and two sharp maxima at around 72° and 135°. These maxima are associated with the deep minima in the $DCS_{\alpha P}^{el}$ ($M_f = 1$) which appear as the denominator in the definition of cos ε. The deviation of cos ε from the value of unity for the theoretical curve is strictly due to the averaging over M_i which causes the loss of coherence between the $M_f = 1$ and $M_f = -1$ scattering amplitudes. For the experimental value, some loss of coherence may also be due to spin-orbit coupling effects and this may account to some extent for the less satisfactory agreement between experiment and theory.

Considering the complexity of the experiments and the fact that the theoretical calculations neglect spin-orbit coupling effects, the general agreement between theory and experiment is surprisingly good for the $E_0 = 20$ eV, $\theta = 10°, 15°, 20°$ cases. This agreement indicates that extended scattering volume effects (see Zetner et al., 1990) are not important in the present measurements and that the CCC calculational scheme, used here, is applicable to elastic scattering by Ba ($^1P_1$) atoms. The rate of convergence and the importance of the ionization channels in our calculations were investigated by also performing calculations with 55 discrete states in the expansion. The results of these calculations were found to be in reasonably good agreement with those described here (which included 115 states and accounted for coupling to the target ionization continuum). The reason for this agreement is that the dipole polarizability for the Ba (6s6p $^1P_1$) state is dominated by the discrete spectrum.

The neglect of spin-orbit coupling in our calculations is justified by the good agreement between experiment and theory. The major effect of spin-orbit coupling in our case manifests itself in singlet-triplet mixing for the target atom. It is well-known, however, that the mixing coefficient for the $^3P_1$ LS term is small (see e.g. Bauschlicher Jr. et al. 1985).

With the assurance given by the good agreement between experiment and theory, we extended the CCC calculations to other scattering angles and impact energies to obtain the various integral elastic scattering and the alignment creation cross sections. Some of these cross sections are listed in Table I, which also shows for purpose of comparison $Q(M_i)$ values as well as experimental and calculated integral elastic scattering cross-sections for ground state Ba atoms at $E_o = 20$ eV. This table shows that alignment can be created by elastic scattering and gives us some indication concerning the magnitude of the alignment creation cross section.

Acknowledgments

The authors acknowledge the financial support by NSF, NASA, NRC and DOE. Support of the South Australian Centre for High Performance Computing and Communications is also acknowledged. We wish to express our gratitude to T. Fujimoto and S. A. Kazantsev for calling our attention to the question of alignment creation in elastic scattering and for valuable discussions. We also acknowledge important communications with P.W. Zetner and D.C. Cartwright.

References

Bauschlicher Jr., C. W., Jaffe, R. L., Langhoff, S. R., Mascarello, F. G. and Partridge, H., 1985 *J. Phys. B,* **18,** 2147.

Dashevskaya E. I. and E. E. Nikitin, E. E., 1987 *Sov. J. Chem. Phys.,* **4** 1934.

Fujimoto, T. (private communication, 1996).

Fursa, D. V. and Bray, I. (to be published, 1998)

Fursa, D. V. and Bray, I., 1997 *J. Phys. B,* **30** 5895.

Kazantsev, S. A. and Henoux, J. C. Polarization Spectroscopy of Ionized Gases, Kluwer Academic Publishers, Dordrecht 1995.

Kazantsev, S. A. (private communication, 1996).

Kazantsev, S. A., Polinovskaya, N. Ya, Pyatritskii, L. N. and Edelman, S. A., 1988 *Sov. Phys. Usp.*, **31** 785.

Macek, J. and Hertel, I. V., 1974, *J. Phys. B,* 7 2173.

Paxio, F. J. de, Padial, N. T., Csanak, Gy. and Blum K. 1980 *Phys. Rev. Lett.*, **41** 749.

Petrashen, A. G, Rebane, V. N. and Rebane, T. K., 1984 *Opt. Spectrosc. (USSR),* **55** 492.

Wang, S., Trajmar, S. and Zetner, P. W., 1994 *J. Phys. B.*, **27** 1613.

Zetner, P. W., Trajmar, S. and Csanak, G., 1990 *Phys. Rev. A,* **41** 5980.

Figure Captions

1. Energy level diagram for Ba. On the right hand side the isotopic and hyperfine structure of the ....6s6p $^1P_1$ level is shown with the energy scale in MHz units.

2. Elastic differential electron scattering cross sections for ^{138}Ba ($^1P_1$) atoms at E_0 = 20 eV. Lines represent the results of CCC calculations. The corresponding experimental values are indicated by symbols. Experimental error limits are also shown.

3. The EICP's (λ and cos ε) for elastic electron scattering by ^{138}Ba ($^1P_1$) atoms at E_0 = 20 eV. • indicates the present experimental results with error limits, the lines are from the present CCC calculations.

Table I. Integral cross sections for elastic electron scattering by ^{138}Ba (...6s6p $^1P_1$) atoms (in 10^{-16} cm^2 units).

	2.8 eV	20.0 eV	97.8 eV
Q (1, 1) = Q (-1, -1)	119.7	36.6	18.1
Q (1, 0) = Q (-1, 0)	2.0	0.74	0.054
Q (1, -1)	4.6	1.6	0.37
Q (0, 0)	89.3	28.5	14.7
Q (0, -1) = Q (0, 1)	1.2	0.62	0.054
$Q(M_f = 0)$	31.1	10.0	4.9
$Q(M_f = 1) = Q(M_f = -1)$	41.8	12.9	6.2
$Q(M_i = 0)$	91.6	30.0	14.8
$Q(M_i = 1) = Q(M_i = -1)$	126.3	39.0	18.5
Q	114.7	35.9	17.3
$Q^{[2]}_{CR}$	8.7	2.4	1.0

$Q(^1S_0 \rightarrow {}^1S_0)$ at E_0=20 eV

Experiment [(a)]: 26.7
CCC calculation [(b)]: 29.4

(a) Wang et al (1994)
(b) Fursa and Bray (1997)

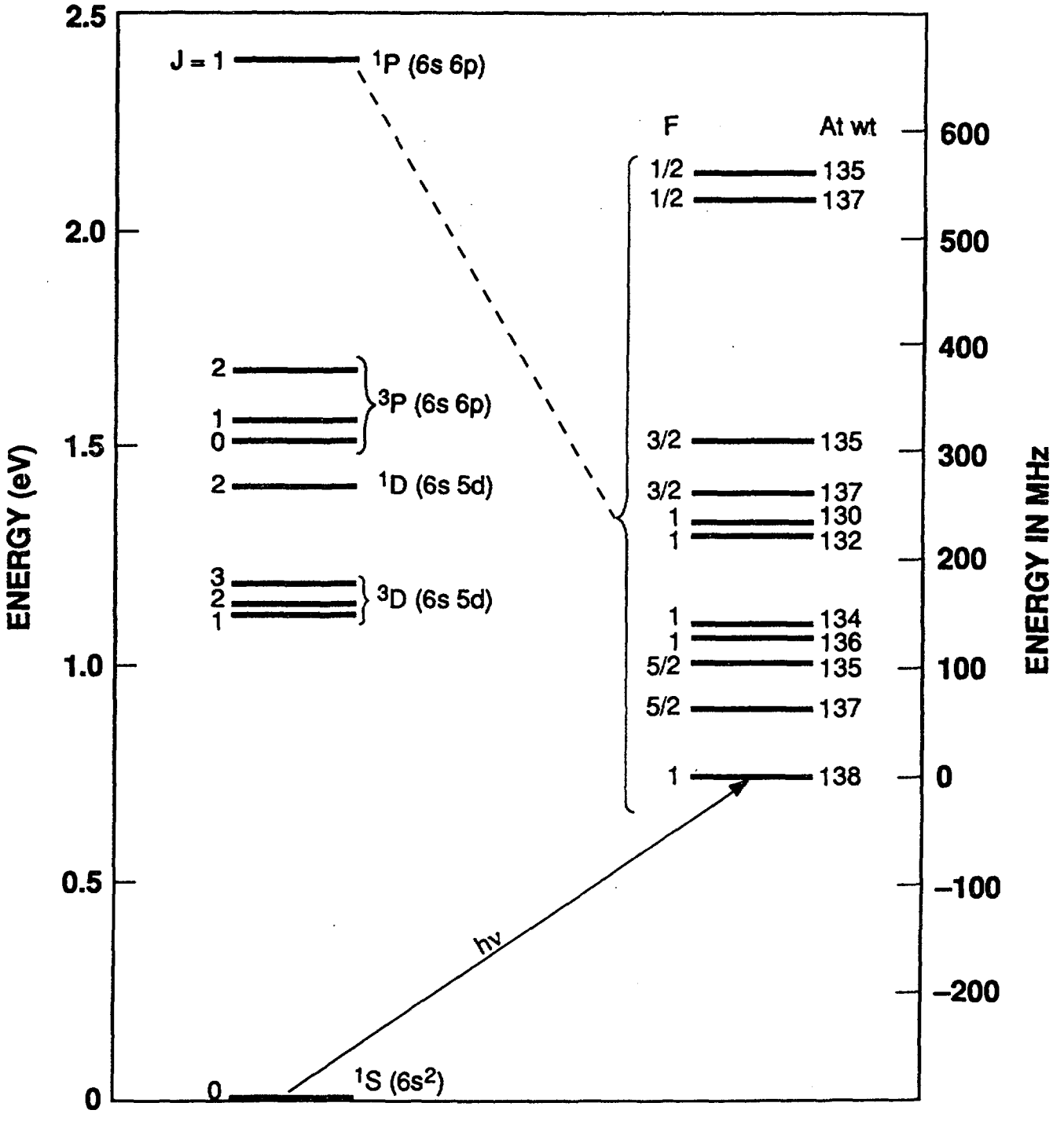
2.5
2.0
1.5
1.0
0.5
0
ENERGY (eV)
J = 1
1P (6s 6p)
2
1
0
3P (6s 6p)
2
1D (6s 5d)
3
2
1
3D (6s 5d)
0
1S (6s2)
hν
F
At wt
1/2
135
1/2
137
3/2
135
3/2
137
1
130
1
132
1
134
1
136
5/2
135
5/2
137
1
138
600
500
400
300
200
100
0
–100
–200
ENERGY IN MHz

Fig. 1

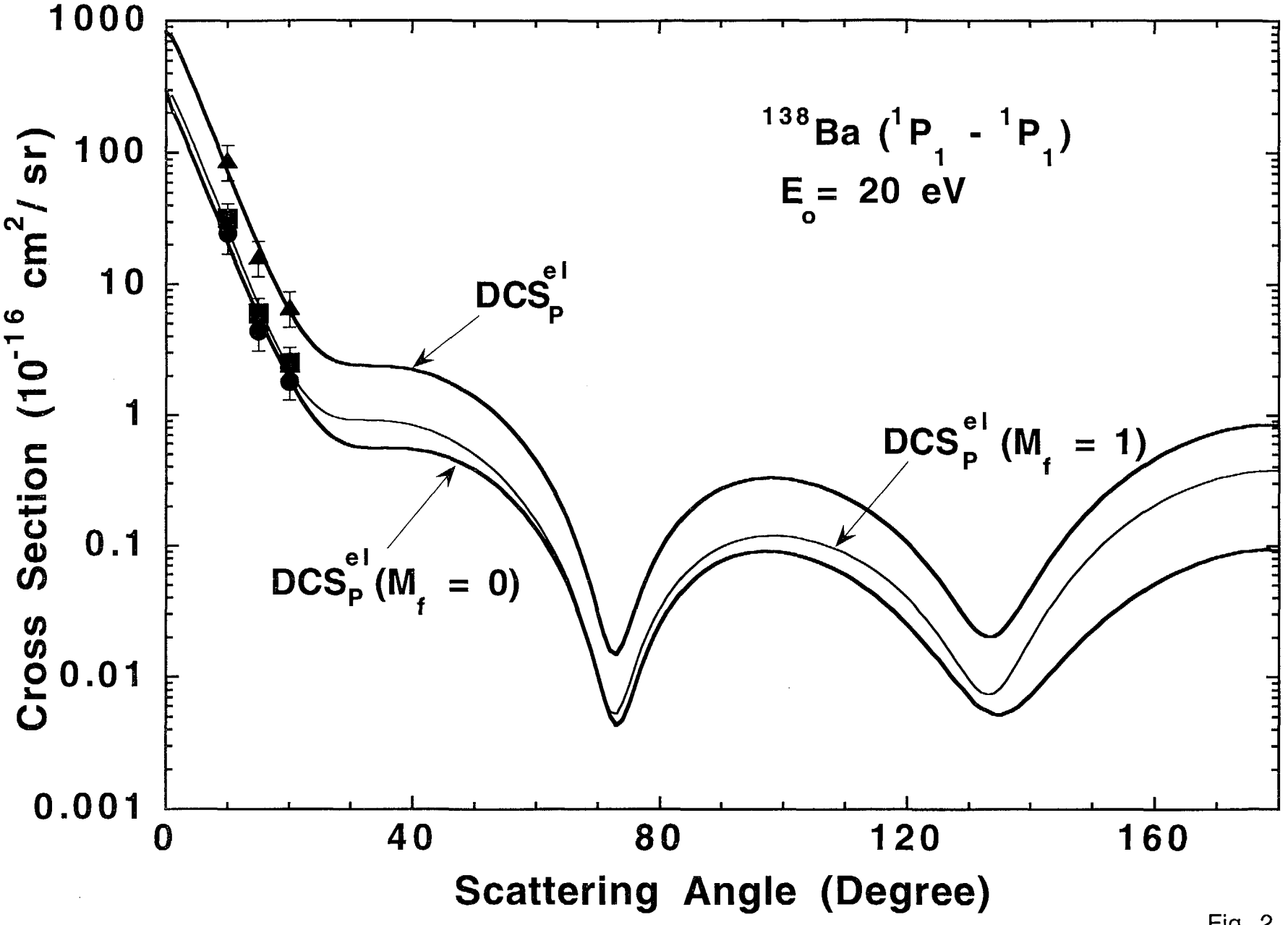
1000
100
10
1
0.1
0.01
0.001
Cross Section (10^{-16} cm^2 / sr)
0
40
80
120
160
Scattering Angle (Degree)
^{138}Ba ($^1P_1$ - $^1P_1$)
E_o = 20 eV
DCS_P^{el}
DCS_P^{el} (M_f = 1)
DCS_P^{el} (M_f = 0)

Fig. 2

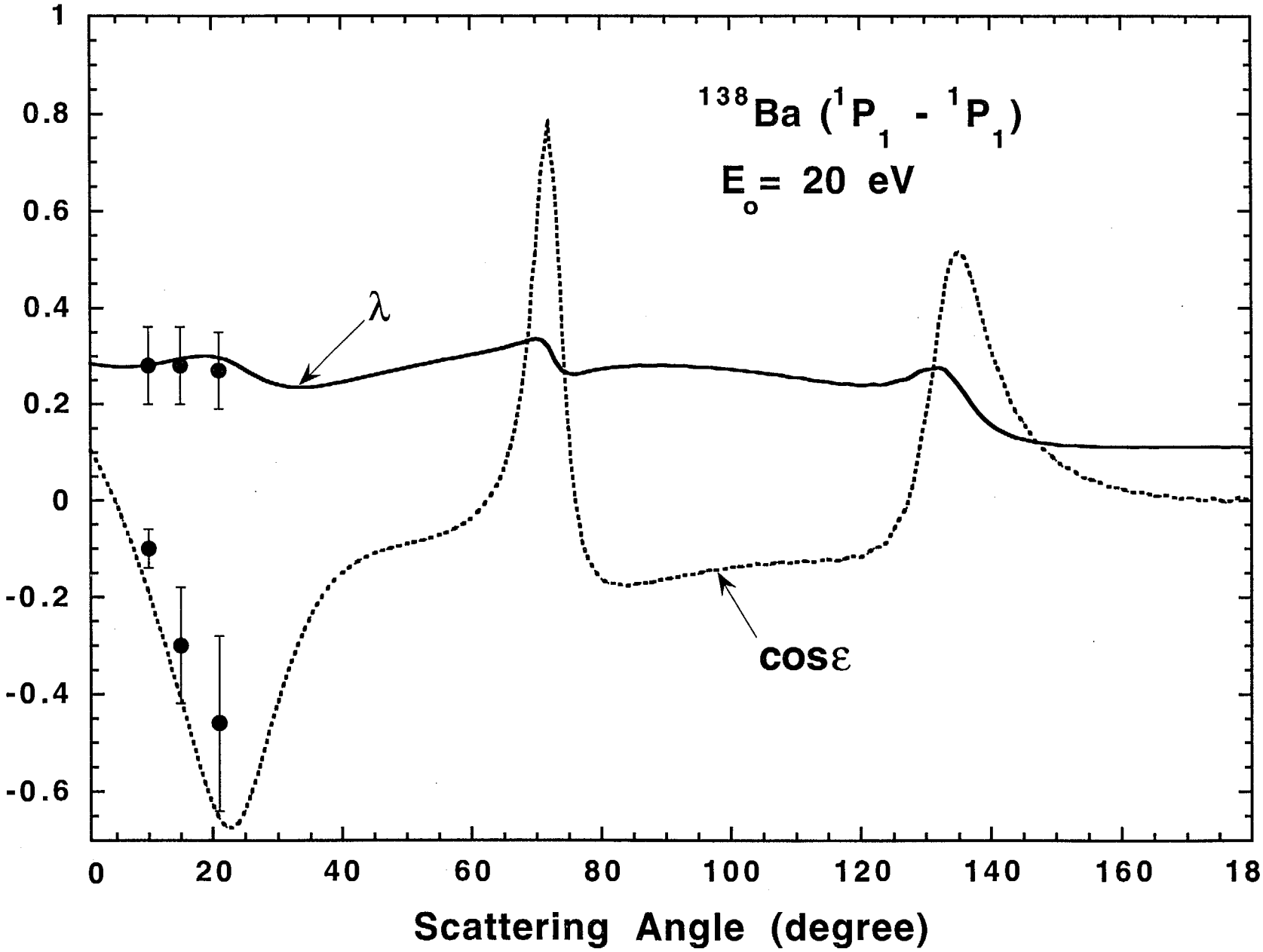
^{138}Ba (^{1}P$_1$ - ^{1}P$_1$)
E$_o$ = 20 eV
λ
cosε
1
0.8
0.6
0.4
0.2
0
-0.2
-0.4
-0.6
0
20
40
60
80
100
120
140
160
180
Scattering Angle (degree)

Fig. 3